

Imidacloprid and thiacloprid neonicotinoids bind more favourably to cockroach than to honeybee $\alpha 6$ nicotinic acetylcholine receptor: Insights from computational studies



Balaji Selvam ^{a,*,**}, Jérôme Graton ^a, Adèle D. Laurent ^a, Zakaria Alamiddine ^a,
Monique Mathé-Allainmat ^a, Jacques Lebreton ^a, Olivier Coqueret ^b,
Christophe Olivier ^b, Steeve H. Thany ^c, Jean-Yves Le Questel ^{a,*}

^a Université de Nantes, UMR CNRS 6230, Chimie Et Interdisciplinarité: Synthèse, Analyse, Modélisation (CEISAM), UFR des Sciences et des Techniques, 2, rue de la Houssinière, BP 92208, 44322 Nantes Cedex 3, France

^b Université d'Angers, Récepteurs et Canaux Ioniques Membranaires, UPRES EA 2647, USC INRA 2023, UFR Sciences, 2 boulevard Lavoisier, 49045 Angers Cedex, France

^c Centre de Recherche en Cancérologie Nantes-Angers, UMR.S 892 – C 6299, Institut de Recherche en Santé IRS Université de Nantes, Unité INSERM 892 – CNRS 6299 Centre de Recherche en Cancérologie Nantes-Angers, 8 quai Moncousu, BP70721, 44007 Nantes Cedex, France

ARTICLE INFO

Article history:

Accepted 31 October 2014

Available online 8 November 2014

Keywords:

nAChRs
Neonicotinoids
Homology model
Docking
Molecular dynamics simulations

ABSTRACT

The binding interactions of two neonicotinoids, imidacloprid (IMI) and thiacloprid (THI) with the extracellular domains of cockroach and honeybee $\alpha 6$ nicotinic acetylcholine receptor (nAChR) subunits in an homomeric receptor have been studied through docking and molecular dynamics (MD) simulations. The binding mode predicted for the two neonicotinoids is validated through the good agreement observed between the theoretical results with the crystal structures of the corresponding complexes with Ac-AChBP, the recognized structural surrogate for insects nAChR extracellular ligand binding domain. The binding site of the two insect $\alpha 6$ receptors differs by only one residue of loop D, a serine residue (Ser83) in cockroach being replaced by a lysine residue (Lys108) in honeybee. The docking results show very close interactions for the two neonicotinoids with both $\alpha 6$ nAChR models, in correspondence to the trends observed in the experimental neonicotinoid-Ac-AChBP complexes. However, the docking parameters (scores and energies) are not significantly different between the two insect $\alpha 6$ nAChRs to draw clear conclusions. The MD results bring distinct trends. The analysis of the average interaction energies in the two insects $\alpha 6$ nAChRs shows indeed better affinity of neonicotinoids bound to $\alpha 6$ cockroach compared to honeybee nAChR. This preference is explained by tighter contacts with aromatic residues (Trp and Tyr) of the binding pocket. Interestingly, the non-conserved residue Lys108 of loop D of $\alpha 6$ honeybee nAChR interacts through van der Waals contacts with neonicotinoids, which appear more favourable than the direct or water mediated hydrogen-bond interaction between the OH group of Ser83 of $\alpha 6$ cockroach nAChR and the electronegative terminal group of the two neonicotinoids (nitro in IMI and cyano in THI). Finally, in both insects nAChRs, THI is consistently found to bind more favourably than IMI.

© 2014 Elsevier Inc. All rights reserved.

1. Introduction

The growing world population and the resulting continuously rising demand in food supply are facing serious threat of crops damages by invertebrate pests. In this context, an important area of sustainable agriculture is the design of potent, selective, efficient and safe insecticides. The modern insecticides should be highly selective of insects over the mammals as well as selective of pests over the beneficial insects such as honeybees. Nicotinic acetylcholine receptors (nAChRs) have shown growing interest for many years and have been recognized as insecticide molecular targets,

Abbreviations: nAChR, nicotinic acetylcholine receptor; Ac-AChBP, *Aplysia californica*-acetylcholine binding protein; LGICs, ligand-gated ion channels; GABA, gamma-aminobutyric acid; 5-HT3, 5-hydroxytryptamine receptor subtype 3; CHARMM, Chemistry at Harvard Molecular Mechanics; IMI, imidacloprid; THI, thiacloprid.

* Corresponding author. Tel.: +33 (0)2 51 12 55 63; fax: +33 (0)2 51 12 55 67.

** Corresponding author. Tel.: +33 (0)2 76 64 51 70; fax: +33 (0)2 51 12 55 67.

E-mail addresses: balaji.panneerselvam@univ-nantes.fr (B. Selvam), jean-yves.le-questel@univ-nantes.fr (J.-Y. Le Questel).

especially for the design of neonicotinoids, classified as agonists of these receptors [1]. Indeed, the role of nAChRs in mediating fast excitatory synaptic transmission in the central nervous system of insects has made them one of the most attractive target for exploration in insecticide discovery [2]. nAChRs belong to the Cys-loop ligand-gated ion channels (LGICs) superfamily, which also includes the GABA, glycine, and 5-HT₃ receptors [3,4]. nAChRs are pentameric LGICs, the five subunits being symmetrically or pseudosymmetrically arranged around a central ion-conducting pore, forming homo- or heteropentamers of related subunits [5,6]. The functional organization of nAChRs, as well as their diversity in terms of subunit composition and stoichiometries, is much better known in vertebrates than in insects [7–9]. The agonist binding site of nAChRs is localized at interfacial regions between subunits and consists of several discontinuous loops (A–F), specific subunit combinations conferring differences in sensitivity to ACh and in pharmacological profiles [5,10]. Rational design of more efficient and selective insecticides would be greatly helped by a high resolution structure of nAChRs. Today, the highest resolution (4.0 Å) structural information on nAChRs comes from electron diffraction of helical tubular crystals of nAChRs from *Torpedo marmorata* [11,12]. In the last years, the determination of the X-ray crystallographic structures of the bacterial transmembrane proteins GLIC (*Gloeobacter violaceus* pentameric ligand-gated ion channel homologue) and ELIC (a bacterial homologue from *Erwinia chrysanthemi*), which are distant homologues of the nAChRs, have revealed many structural features of these membrane proteins, notably the architecture of the pore, including its gate and its selectivity filter [3,13–15]. However, these structures do not allow a comprehensive description of the ligand–nAChRs interactions.

In this context, the discovery and crystallization of ligand-free and ligand-bound structures of acetylcholine binding protein (AChBP) have allowed to gain deep insights into the details of the binding site and its relation to function [16–22]. In the field of insecticides, AChBP extracted from *Aplysia californica* (Ac-AChBP) has been used as a plausible structural surrogate of insects nAChRs because it has been shown to be pharmacology reminiscent for the insect nAChR subtypes, that is, to present high neonicotinoid sensitivity [23]. These data have provided the structural basis for the design of homology models for extracellular domains of specific nAChRs subunits combinations and the investigation of the binding of neonicotinoids on the corresponding receptor–ligand binding interfaces [24]. Considering the fact that the exact composition of the sensitive nAChRs is still unknown, various nAChRs isoforms from different insect species have been already considered: e.g. $\alpha 2\beta 1$, $\alpha 1\beta 2$ from peach potato aphid (*Myzus persicae*) and honeybee (*Apis mellifera*) [2,22,24–27].

From an experimental point of view, several studies combining binding assays, molecular biology and electrophysiology have investigated the sensitivity of various nAChRs subtypes to neonicotinoid insecticides [27–32]. However, these studies have been hindered by difficulties encountered in expressing recombinant insect nicotinic receptors leading to functional recombinant nAChRs. A number of strategies was developed to overcome such difficulties and, only experimental data have been obtained for *Drosophila* nAChR subunits D α 5 and D α 7 [32] and Nl α 1 and Nl α 2 subunit of brown planthopper *Nilaparvata lugens* [33]. Within this framework, the expression of functional recombinant nAChRs has been reported for several insect nAChR α subunits and co-expressed with vertebrate β subunits [33,34].

In the present work, we have investigated through complementary molecular modelling methods the binding of imidacloprid (IMI) and thiacloprid (THI), two important neonicotinoids, to homomeric $\alpha 6$ nAChRs of cockroach (*P. Americana*) and honeybee (*A. mellifera*). It is worth noticing that we have limited the modelling of nAChRs to the isolated extracellular domains (ECD) rather than

considering the full-length nicotinic acetylcholine receptor. We have selected the $\alpha 6$ subunits because they have strong sequence similarity with $\alpha 5$ and $\alpha 7$ nAChRs subunits of the *Drosophila* insect model that have been proven to form functional homomeric and heteromeric ion channels [33]. The consideration of homomeric species obviously simplifies the pentameric nAChR model. By selecting cockroach and honeybee nAChRs, our objectives are (i) to rationalize at the atomic level the binding of IMI and THI in the targeted nAChRs and (ii) to draw guidelines for the development of new compounds selective of pests with respect to honeybees. Actually, IMI and THI neonicotinoids are the only two representatives of this class of insecticides for which crystallographic data are available and accurately describe the specific interactions with Ac-AChBP at the atomic level [35]. Therefore, these structural data allows us to check *a posteriori* the validity of the receptor–ligand complexes built from the homology models. After a discussion on the homology models, the docking results are presented and compared for the neonicotinoids in each targeted nAChRs ($\alpha 6$ cockroach and $\alpha 6$ honeybee). A comparison of the binding interactions observed for the two insecticides in the two insect species nAChRs is carried out from these results. Significant differences in terms of the nature of the interactions and their geometric features are obtained. Molecular dynamics simulations have then been realized to complete these data. These analyses provide key elements rationalizing the behaviour of both neonicotinoids with respect to the targeted nAChRs and could be used for the rational design of new compounds with a better efficiency and selectivity.

2. Methods

2.1. Homology modelling

The amino acid sequences of the cockroach *P. americana* and honeybee *A. mellifera* $\alpha 6$ subunits were extracted from the Uniprot server (www.expasy.org) [36]. The closest homology of the target sequences were identified using the BLAST programme [37]. The crystal structure of the acetylcholine binding protein (Ac-AChBP) extracted from *A. californica* (Ac) (PDB ID: 3C79) [24] was selected as a template to build the three-dimensional (3D) model of cockroach and honeybee nAChRs. Indeed, Ac-AChBP is the recognized surrogate for the ligand binding domain of the extracellular domain of insect nAChRs [38]. The crystal structures of the Ac-AChBP–neonicotinoid complexes (PDB ID: 3C79 and PDB ID: 3C84 for IMI and THI ligands, respectively) were downloaded from the Protein Data Bank (www.pdb.org) [39]. The pairwise sequence alignments were performed to align the target and the template sequence. The 3D homology models were built using the Prime v3.6 [40] module of the Schrodinger suite 2014-1 [41]. The rotamers of the conserved amino acid residues are preserved in the homology model such that the final 3D model does not significantly deviate from the template structure. The stereochemical quality of the model was verified using MolProbity (Figs. S1 and S2) [42].

2.2. Docking

The chemical structures of IMI and THI neonicotinoids are shown in Fig. 1. The structures have been converted to 3D at pH 7.0 ± 0.2 using the LigPrep v3.0 [43] module of the Schrodinger suite 2014-1 [10]. The 3D ligand molecules were then subjected to the confgen [44] programme to retrieve the lowest energy conformer for docking. The docking was performed using the Glide v6.3 [45] programme of the Schrodinger suite 2014-1 [10]. The residues around 6 Å of the ligand were defined as the active site and were selected for the receptor grid generation. The extra-precision (XP) [46] mode of the docking algorithm was employed to dock IMI and

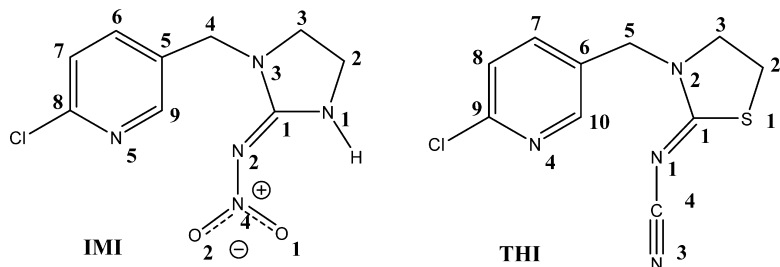


Fig. 1. Imidacloprid (IMI) and thiacloprid (THI) chemical structures.

THI ligands. The wincoot 0.7.2.1 crystallographic refinement software has been used to assess the probability of conformation of the various binding site residues, in particular of the non-conserved lysine residue. This analysis has led to a probability of conformation of the lysine residue of 88%. For the sake of comparison, we have also used the SCWRL software, which predicts for lysine a conformation similar to our model, with a corresponding probability of 88%. Fig. S3 (SI) compares the results of the various approaches used to investigate the conformational features of the binding site residues. It is worth reminding that nAChRs are organized as pentamers; that is, there are five identical ligand binding sites and the ligand binds between the cleft of the two subunits. The ligands were therefore docked in all the five subunits of both nAChRs models. The docking results were validated by comparing the predicted ligand binding modes to the crystallographic Ac-AChBP-neonicotinoid structures. Furthermore, the binding of IMI and THI neonicotinoids to cockroach and honeybee $\alpha 6$ homo-pentamers have been analyzed from the glide energies and the docking scores. The glide energy is the summation of total electrostatic (Coulombic) and van der Waals terms for protein–ligand interactions in a given complex whereas the docking scores are estimate of the ligands binding energies. The latter are of course approximate values and have to be interpreted with caution, but both parameters are generally considered when comparing docking results.

2.3. Molecular dynamics simulations

All-atom molecular dynamics (MD) simulations were performed using DESMOND v3.8 [47] with the CHARMM27 force field for the protein and the neonicotinoids [48]. The protein–ligand complexes were solvated using the System Builder panel in Maestro 9.7 [49] with SPC water molecules in an orthorhombic periodic box of $100 \text{ \AA} \times 100 \text{ \AA} \times 100 \text{ \AA}$ dimension. A total of 67 sodium and chloride ions were added to neutralize the system, the final model having approximately 90 000 atoms. In the first step, the MD system was energy minimized using a conjugate gradient algorithm for 2000 iterations up to a convergence value of $1.0 \text{ kcal/mol}/\text{\AA}$. In the second step, the MD system was slowly heated to 10 K in isochore conditions (NVT) over 12 ps and later heated to 300 K in isothermal-isobaric ensemble (NPT) over 12 ps. The protein–ligand complex system was equilibrated for 7 ns and then the production runs were carried out up to 40 ns. The Particle-Mesh Ewald [50] method was used for the calculation of the electrostatic interactions and the SHAKE algorithm [51] was used to constrain the bonds. The temperature was kept constant at 300 K by a Berendsen thermostat. For each system (cockroach and honeybee nAChRs), a total of six individual simulations of $\alpha 6$ homo-pentamers were carried out with four different initial velocities over a period of 40 ns. These simulations correspond to the complexes with IMI and THI in each subunit interface of the two $\alpha 6$ nAChRs (total of twenty simulations) and to the apo structures (two simulations). For the sake of comparison and to check the quality of the final models, the average neonicotinoid–nAChR MD structures have been compared to

the corresponding neonicotinoid–Ac-AChBP crystallographic structures through the calculation of RMSDs taking into account, for the protein, the backbone atoms and for the neonicotinoids the heavy atoms. The pairwise interaction energies were calculated by selecting the ligand molecule and the respective binding site residues. The default DESMOND values were used as cutoff distances for the various interactions: hydrogen-bond $\leq 2.5 \text{ \AA}$, aromatic $\leq 4.5 \text{ \AA}$ and hydrophobic $\leq 3.6 \text{ \AA}$.

3. Results and discussion

3.1. Homology modelling

The pairwise sequence alignments of the extracellular domain of the cockroach and honeybee $\alpha 6$ nAChR subunits against the template crystal structure (PDB ID: 3C79) [24] show 27.4% and 29% identity and 44.7% and 45.1% similarity, respectively (Fig. 2A and B). The sequence identity value is below the 30% “threshold” for high accuracy template-based 3D modelling. However, despite this relatively low level of sequence identity, accurate alignment can be obtained in this case as reflected by the relatively high sequence similarity value. This is because membrane proteins provide a highly contrasted environment with a hydrophobic internal region and hydrophilic edges imposing a strict conservation of residues, conservation of apolar and polar segments [52]. Based on the sequence alignments, the 3D models of cockroach and honeybee $\alpha 6$ nAChR homo-pentamers were built using the Prime module [9] of the Schrodinger suite 2014-1 [10] (Figs. 3 and 4). The generated models were energy minimized using the OPLS-2005 force field [53]. The quality of the 3D model in terms of geometry was assessed using the MolProbity programme [42]. Both the final models showed 99.6% residues (except proline and glycine residues) possess their ϕ , ψ torsional angles in the most energetically favoured regions of the Ramachandran plot [54]. The protein backbone root mean square deviations (RMSD) of the final cockroach (Fig. 3A) and honeybee (Fig. 4A) $\alpha 6$ models are respectively of 0.42 \AA and 0.37 \AA , using the template structure (3C79) as the reference and no deviation was observed in the important loops within the binding site.

3.2. Docking

In order to investigate the impact of the differences in the binding site between the two species in their interactions with neonicotinoids, we docked IMI and THI neonicotinoids in the cockroach and honeybee $\alpha 6$ nAChRs. The amino acid composition of the ligand binding site of cockroach and honeybee nAChRs shows 92.3% identity and differs by one residue located in loop D (Fig. 5). More precisely, the Ser83 of loop D in cockroach $\alpha 6$ nAChR is replaced by Lys108 in honeybee (Fig. 6). The equivalent residue in the Ac-AChBP crystal structure [24] is Gln57. This latter residue has been shown to be involved in neonicotinoid Ac-AChBP binding by recognizing IMI through the formation of a direct hydrogen bond with the IMI

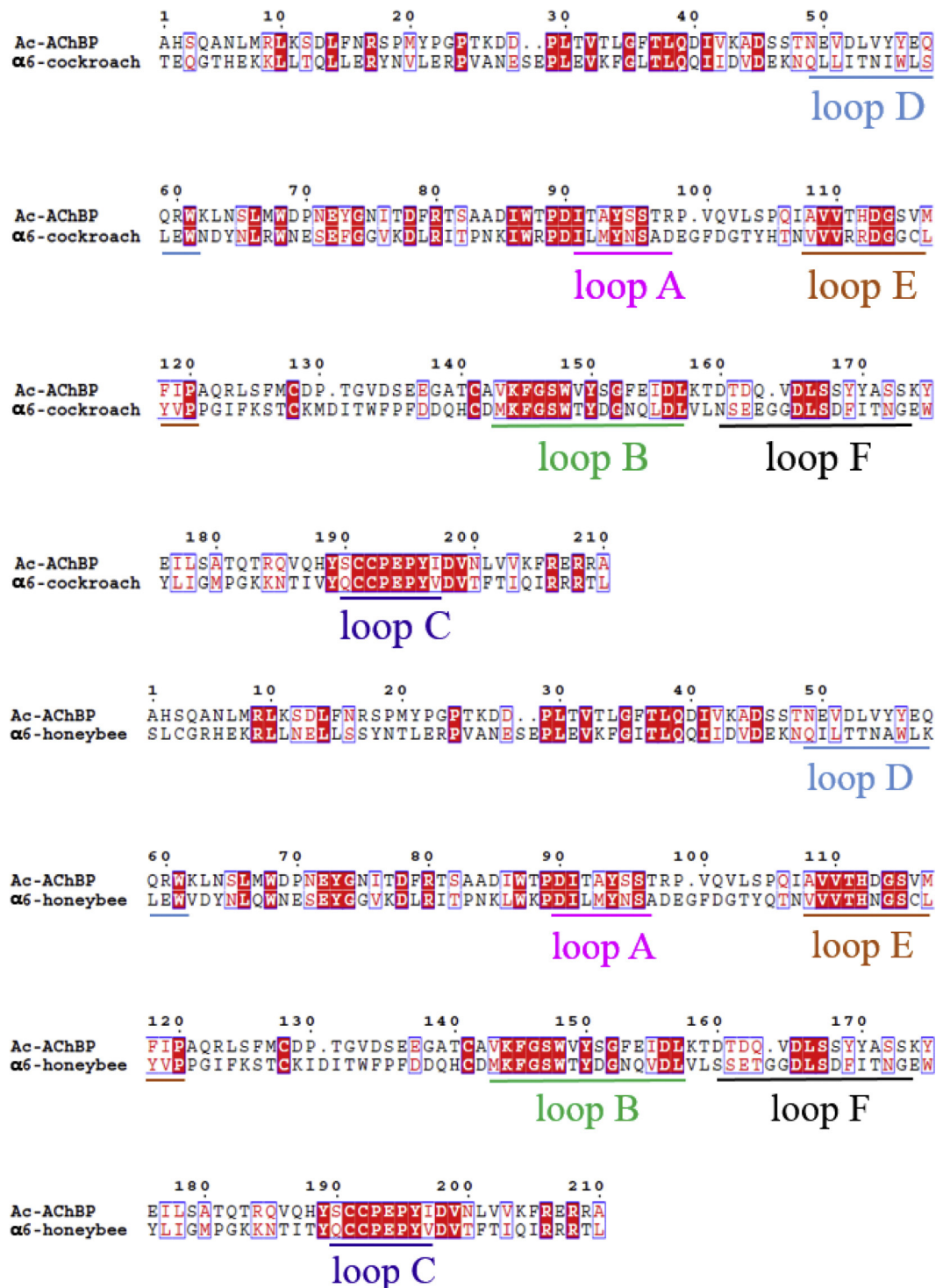


Fig. 2. (A) Sequence alignments of Ac-AChBP and $\alpha 6$ cockroach nAChRs used to generate the $\alpha 6$ cockroach nAChR homology model. (B) Sequence alignments of Ac-AChBP and $\alpha 6$ honeybee nAChR used to generate the $\alpha 6$ honeybee nAChR homology model.

terminal nitro group and forms also bridged contacts with the cyano group of THI [24]. As explained in the methodology section, the ligands were docked in all five subunits of both nAChRs. The docking results show that both IMI and THI neonicotinoids bind similarly, as observed in the neonicotinoid–Ac-AChBP crystal structures 3C79 [24] (IMI) and 3C84 [24] (THI). The same trends have been observed in all five interfaces and only the results obtained for one of the subunit (AB) will therefore be presented and discussed here. The binding modes of IMI and THI in the AB subunit interface for both $\alpha 6$ nAChR models are shown in Fig. 6.

The geometric parameters, docking scores and glide energy for the interactions of the two neonicotinoids in the AB subunit interfaces of the two nAChRs are listed in Table 1. The docking scores and glide energy of the top ranked poses show that the ligands bind more tightly in cockroach than in honeybee nAChR. Furthermore, many specific interactions between the ligand and the binding site residues are similar in both species. The pyridine ring of the neonicotinoids forms respectively π – π interactions with Trp175 and Trp200 of the cockroach and honeybee nAChRs. The nitro group of IMI is involved in a hydrogen-bond (H-bond) interaction with the

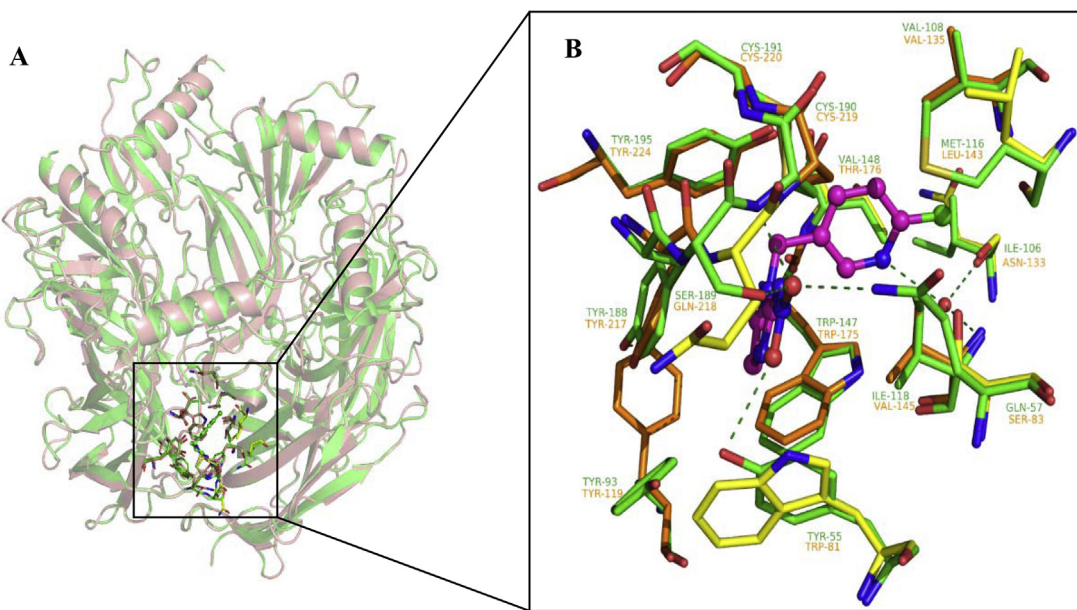


Fig. 3. (A) Superposition of α_6 cockroach nAChR homology model (orange) on the 3C79 (green) crystallographic structure. (B) View of the binding site residues for one of the subunit interfaces of α_6 cockroach (orange) and 3C79 (green). The non-conserved residues are represented in yellow. The pictures were generated with Pymol v0.99. (For interpretation of reference to color in this figure legend, the reader is referred to the web version of this article.)

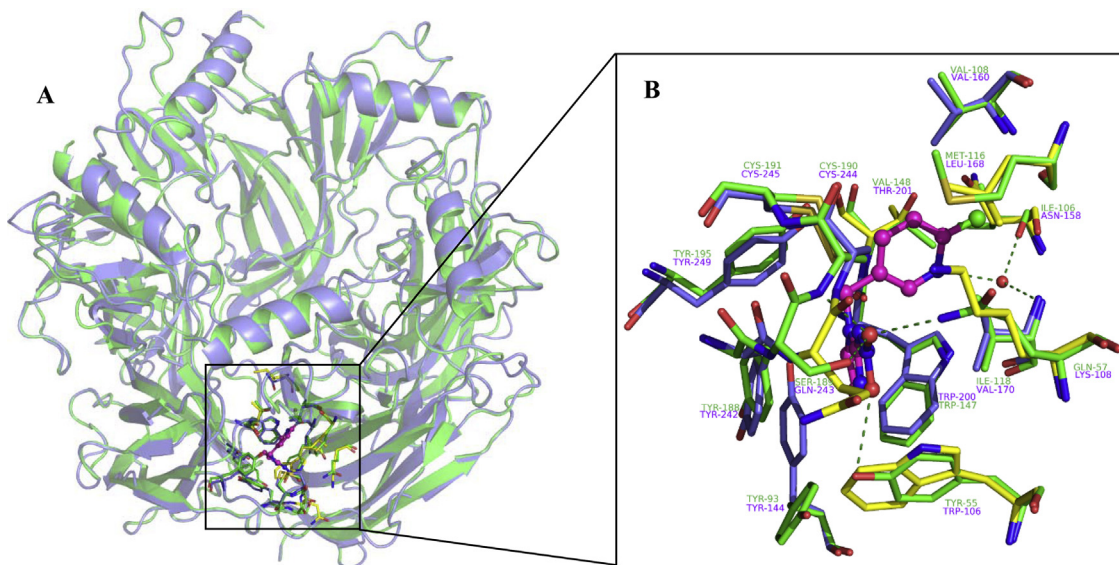


Fig. 4. (A) Superposition of α_6 honeybee nAChR homology model (blue) on the 3C79 (green) crystallographic structure. (B) View of the binding site residues for one of the subunit interfaces of α_6 honeybee (blue) and 3C79 (green). The non-conserved residues are represented in yellow. The pictures were generated with Pymol v0.99. (For interpretation of reference to color in this figure legend, the reader is referred to the web version of this article.)

Table 1

Docking scores and glide energies of IMI and THI in α_6 cockroach and honeybee nAChRs (AB subunits interface). The docking scores and glide energies computed for the other subunits are listed in Supporting Information (Tables S1 and S2).

nAChR	Neonicotinoid	DH · A	d(DH · A)	DS	GE	RMSD
α_6 Cockroach (AB subunits interface)	IMI	NH _(Trp81) ^{SC} ···O _(NO2)	2.57			
		OH _(Ser83) ^{SC} ···O _(NO2)	2.98			
		NH _(Gln218) ^{MC} ···O _(NO2)	2.73	-7.06	-62.02	0.90
		NH _(Cys219) ^{MC} ···O _(NO2)	3.02			
α_6 Honeybee (AB subunits interface)	THI	NH _(Trp81) ^{SC} ···N _{3(CN)}	2.43			
		OH _(Ser83) ^{SC} ···N _{3(CN)}	3.31			
	IMI	NH _(Trp106) ^{SC} ···O _(NO2)	2.58			
		NH _(Gln243) ^{SC} ···O _(NO2)	2.72	-6.07	-69.83	1.41
	THI	NH _(Cys244) ^{SC} ···O _(NO2)	2.85			
		NH _(Trp106) ^{SC} ···N _{3(CN)}	2.31	-6.62	-60.07	1.15

DH: H-bond donor; A: H-bond acceptor; d: H-bond distance (\AA); DS: docking score; GE: glide energy (kcal/mol); RMSD: root mean square distance (\AA) of the neonicotinoid docking poses with respect to the experimental crystallographic structure; MC: main chain of the residue; SC: sidechain of the residue.

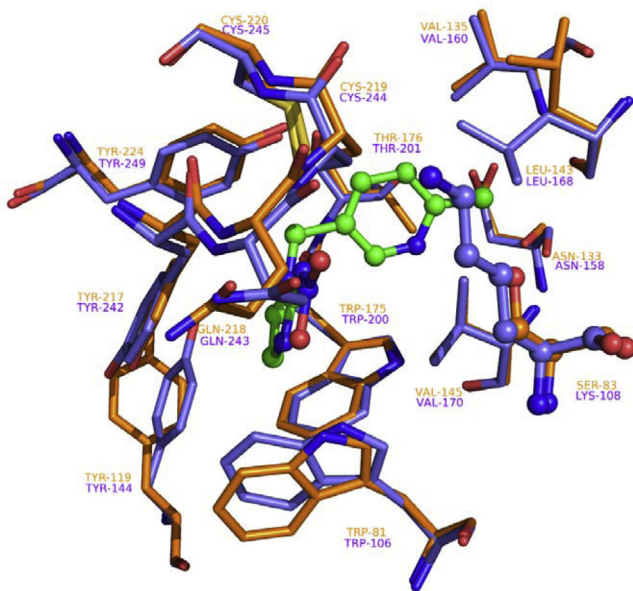


Fig. 5. Comparison of the binding sites of α_6 cockroach and honeybee nAChRs. The experimental binding mode of IMI has been extracted from the Ac-AChBP crystal structure and shown in green. For clarity, the ligand and the non-conserved residues are represented in ball and sticks. (For interpretation of reference to color in this figure legend, the reader is referred to the web version of this article.)

side chain NH groups of the Trp81 (cockroach) and Trp106 (honeybee) residues in both nAChRs. The backbone NH groups of Gln218 and Cys219 of cockroach and Gln243 and Cys244 of honeybee nAChRs also interact with the nitro group of IMI. In contrast to IMI, the THI ligand does not form any interaction with the residues of loop C as its cyano group is linear and lies towards the complementary chain of the subunit. However, in the Ac-AChBP crystal structure, H-bond interactions were observed between the neonicotinoid and the residue Ser189 of loop C through water molecules [24]. Additionally, the IMI and THI ligands make an extra H-bond with the non-conserved Ser83 in cockroach α_6 receptor. Conversely, the corresponding Lys108 of honeybee α_6 receptor does not form any interaction with either neonicotinoids. To confirm these trends, we have performed induced fit docking, which allows full relaxation of the residues located at 5 Å of the ligand during the docking, followed by a final energy minimization of the docked poses. The lowest energy conformation of the top ranked docked pose resulting from this approach doesn't present any interaction between Lys108 and the neonicotinoids. Indeed, some poses predicted by the docking show Lys108-neonicotinoid interactions but the probability of existence of these lysine conformations are very poor as the preferred conformations of Lys108 are elongated/stretched rather than folded ones. Therefore, the formation of specific interactions such as H-bonding ones with Ser83 might increase the affinity of neonicotinoid binding towards the cockroach α_6 nAChR compared to honeybee α_6 receptor. However, experimental studies have shown that despite the least number of interactions of THI in the two nAChRs compared to IMI suggested in the present work, its affinity appears better [55,56]. These trends must therefore be considered cautiously since the docking scores and glide energies obtained for the two neonicotinoids are very close.

3.3. Molecular dynamics simulations

To gain more insight into the role of (i) non-conserved residues and (ii) water molecules in the binding of IMI and THI neonicotinoids to cockroach and honeybee α_6 nAChRs, molecular dynamics (MD) simulations were performed.

3.3.1. Global motion

The MD trajectories of four different runs were analyzed for all subunit interfaces. Since the results obtained from multiple trajectories show similar trends for all subunits, only one (AB subunit interface) will be discussed in detail. The dynamic flexibility of the MD systems has been assessed by measuring the root mean square deviations (RMSD) of C α atoms. The RMSD plots indicate that the apo structures of cockroach and honeybee nAChRs fluctuate more than the ligand bound complexes (Fig. 7). The MD system of apo structures exhibits higher RMSD until 12 ns and reaches equilibrium after 15 ns. For ligand bound complexes, the RMSD increases until 10 ns and converges around 12 ns. It is worth noticing that the flexibility pointed out by the MD simulations is in line with the affinity trends found through the docking results. Thus, the apo forms appear more flexible, followed by the neonicotinoids–honeybee α_6 and –cockroach α_6 complexes, the cockroach being the least flexible. We have also calculated root mean square fluctuation (RMSF) values of the active site residues in order to determine the ligand-induced conformational changes over the simulation time (Fig. S4). The RMSD and RMSF values are consistent with each other and in agreement with the previous trends: the complexes of the two neonicotinoids appear systematically more flexible for honeybee compared to cockroach nAChRs. Furthermore, the THI complexes are shown to be less flexible than the IMI ones in both cases (Fig. S5), a behaviour in agreement with the trends suggested by the experimental studies mentioned above.

3.3.2. Neonicotinoid–nAChR binding site interactions

At first, we have investigated the timelines of the neonicotinoid–nAChR interaction energy for the four systems selected for discussion (IMI and THI in the AB interface of α_6 cockroach and honeybee nAChR) in order to investigate for each neonicotinoid–nAChR system the evolution of the interaction energy. The energy plots reported in Fig. 8 show, on average, more favourable binding energies of neonicotinoids for cockroach than for honey bee α_6 nAChRs. From a structural point of view, we have compared the four average neonicotinoid–nAChR MD structures selected for discussion to the corresponding neonicotinoid–Ac-AChBP experimental structures through RMSD measurements (Fig. S6). This approach has led to RMSDs of 1.71 and 1.32 Å, respectively, for IMI complexes with α_6 cockroach and honeybee nAChRs taking the 3C79 PDB entry as reference, corresponding values of 1.25 and 1.16 Å being obtained for THI complexes with α_6 cockroach and honeybee nAChRs taking the 3C84 PDB entry as reference. These values validate our models since they are significantly below the 2.00 Å value generally considered as the upper limit for validation of binding poses.

For a better characterization of the neonicotinoid–nAChR complexes and to determine the relative contribution of the cockroach and honeybee α_6 nAChRs amino acid residues in the binding site of IMI and THI, the behaviour of the various molecular interactions such as direct and water-mediated H-bonds, π – π and van der Waals contacts along the simulation time has been analyzed. The nitrogen atom of the pyridine ring of the two neonicotinoids (N5 and N4 in IMI and THI, respectively) is consistently involved in water-mediated interactions in both nAChRs. The average interaction profiles of IMI and THI with binding site residues of cockroach and honeybee α_6 nAChR are shown in Fig. 9. This H-bond interaction is stable in both α_6 models. It is observed over 87% and 85%, and 79% and 81% of the simulation times in cockroach and honeybee nAChR complexed with IMI and THI, respectively. These results are in good agreement with the previous studies on the role of water molecules being in close interaction with the ligands in Ac-AChBP [57]. Indeed, it has been shown that this interaction is further stabilized by H-bonds with the backbone NH group of Leu112 and the sidechain NH group of Trp143 in AChBP. These results are also in line with the functional role of water molecules

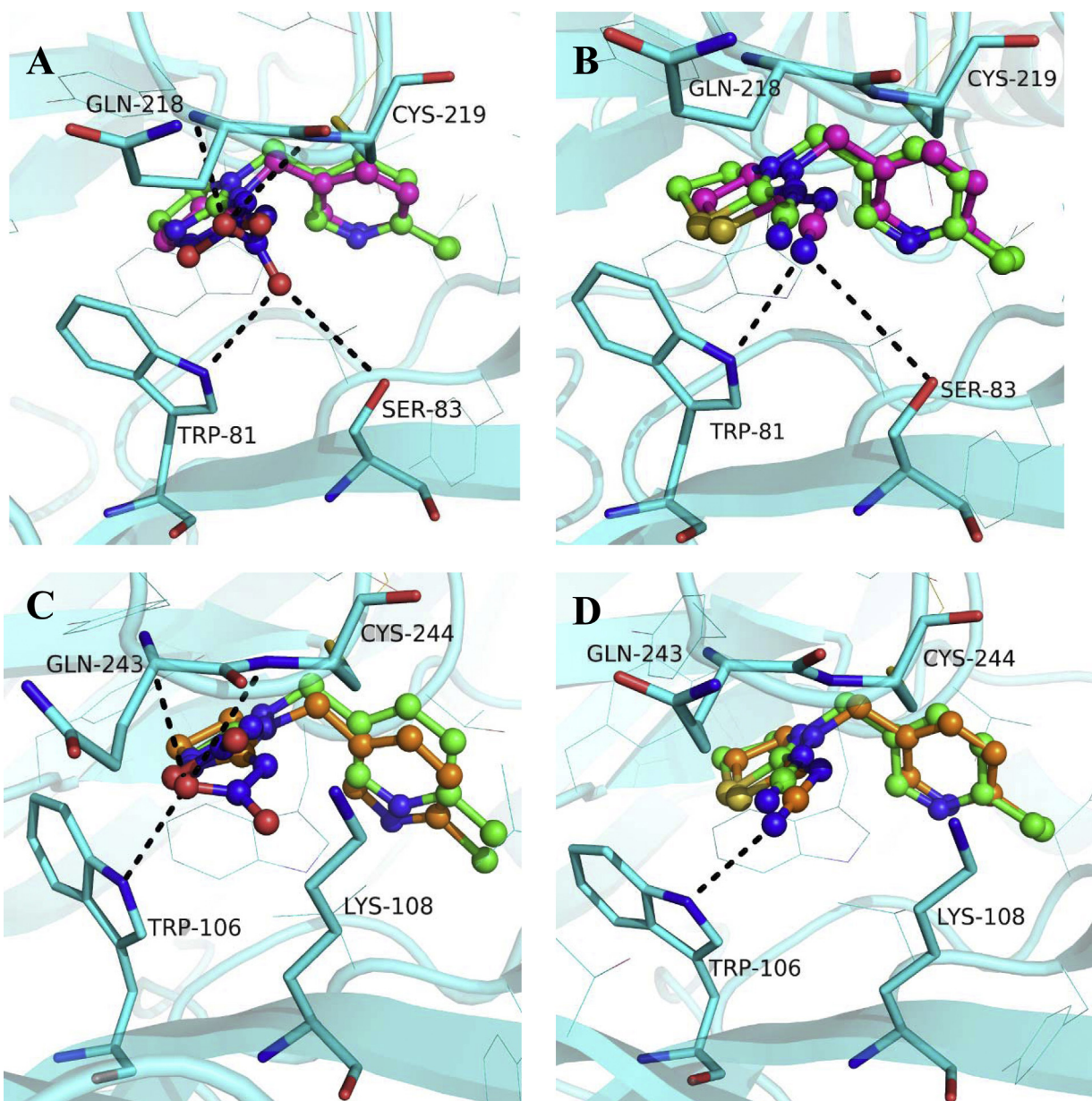


Fig. 6. Predicted binding modes of IMI (A) and THI in $\alpha 6$ cockroach (B) and honeybee nAChRs (C: IMI and D: THI). The crystal structure binding modes of IMI and THI in Ac-AChBP are shown in green and used as a reference for the validation of the docking protocol.

in the binding of neonicotinoid derivatives to nAChRs suggested through molecular modelling and structure activity relationship (SAR) studies [58]. The push-pull pharmacophore of IMI and THI forms direct H-bonds as well as water-mediated contacts with Trp81/106 and Cys219/244 residues of the cockroach and honeybee nAChRs. The nitro group of IMI interacts with NH sidechain indole ring of Trp81 and Trp106 with respective occupancies of 69% and 48% in cockroach and honeybee nAChRs. The nitro group also establishes less stable H-bond interactions with backbone NHs of Cys219 and Cys244 (relatively 36% and 21%, respectively, in the two nAChRs).

From a ligand chemical structure point of view, the V-shaped nitro group of IMI is replaced by a linear cyano group in THI and appears to make stronger contacts with the binding site residues. The H-bond between the C≡N group of THI and the sidechain NH group of Trp81 is found to be more stable in cockroach than in honeybee nAChR on the basis of the corresponding frequencies of occurrence. Indeed, this hydrogen bond is present 74% of the total

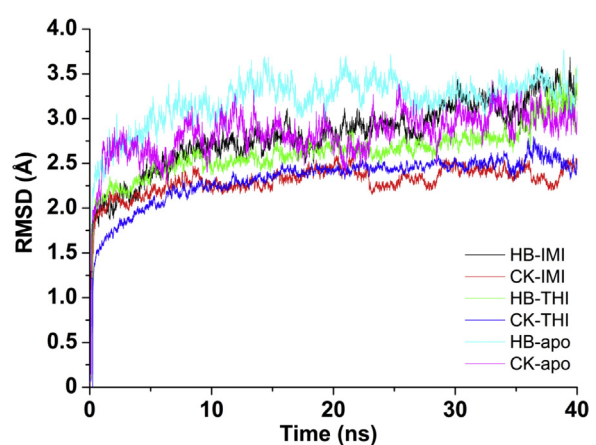


Fig. 7. RMSD plot of C α atoms versus the simulation time.

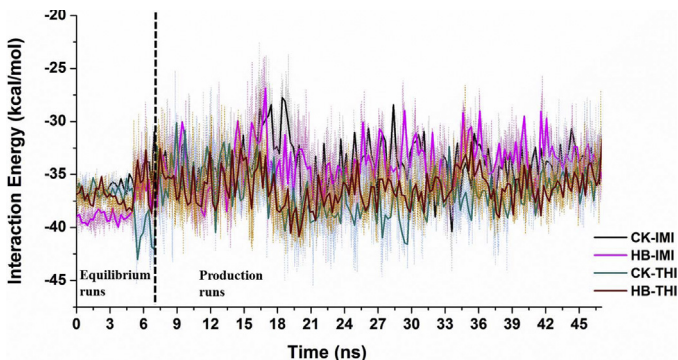


Fig. 8. Interaction energy plot along the simulation time for the four neonicotinoid- α_6 nAChR complexes considered.

simulation time compared to 43% in honeybee nAChR. The ligand also forms water-mediated contacts with main chain NH groups of Cys219 and Cys244 of cockroach and honeybee nAChRs with 11% and 6%. These frequencies of H-bond interaction are significantly lower than those obtained for IMI in both nAChRs (36% cockroach and 21% honeybee nAChR). Nevertheless, these data are in agreement with the water-mediated contact observed between the nitrile group of THI and the Cys190 main chain NH of loop C [24]

in the THI-Ac-AChBP crystal structure. The non-conserved Ser83 residue recognizes the neonicotinoids through direct and water-mediated contacts. The Ser83 interacts with the nitro and cyano groups of the respective ligands with occupancy of 11% and 8% over the simulation time. In contrast, the equivalent residue (Lys108) in honeybee nAChR interacts less than 1% with the neonicotinoids.

The non-bonded and aromatic interactions established in the agonist nAChRs binding site play a major role in stabilizing the bounded conformations of IMI and THI. The aromatic residues Trp175 and Trp200, in cockroach and honeybee α_6 nAChRs respectively, form face-to-edge stacking interactions with the two neonicotinoids. This particular aromatic interaction becomes very persistent and presumably strong over the course of the simulation with occupancies of 78% and 81%, and 73% and 69% in cockroach and honeybee nAChRs complexed with IMI and THI, respectively. The two aromatic residues Tyr217/242 and Tyr224/249 of loop C anchors the ligand in the requisite conformation through hydrophobic interactions in both receptors. These interactions appear to be more specific for the ligands in cockroach nAChR compared to honeybee. The phenyl ring of Tyr217 in cockroach nAChR interacts with imidazolidine and thiazolidine part of IMI and THI with average occupancies of 68% and 63%. In contrast, the interaction is slightly less pronounced in honeybee nAChR, with average occupancies of 59% and 51%, respectively, for both neonicotinoids. Tyr224 and Tyr249 also form similar hydrophobic interactions with the two neonicotinoids bound with cockroach and honeybee α_6

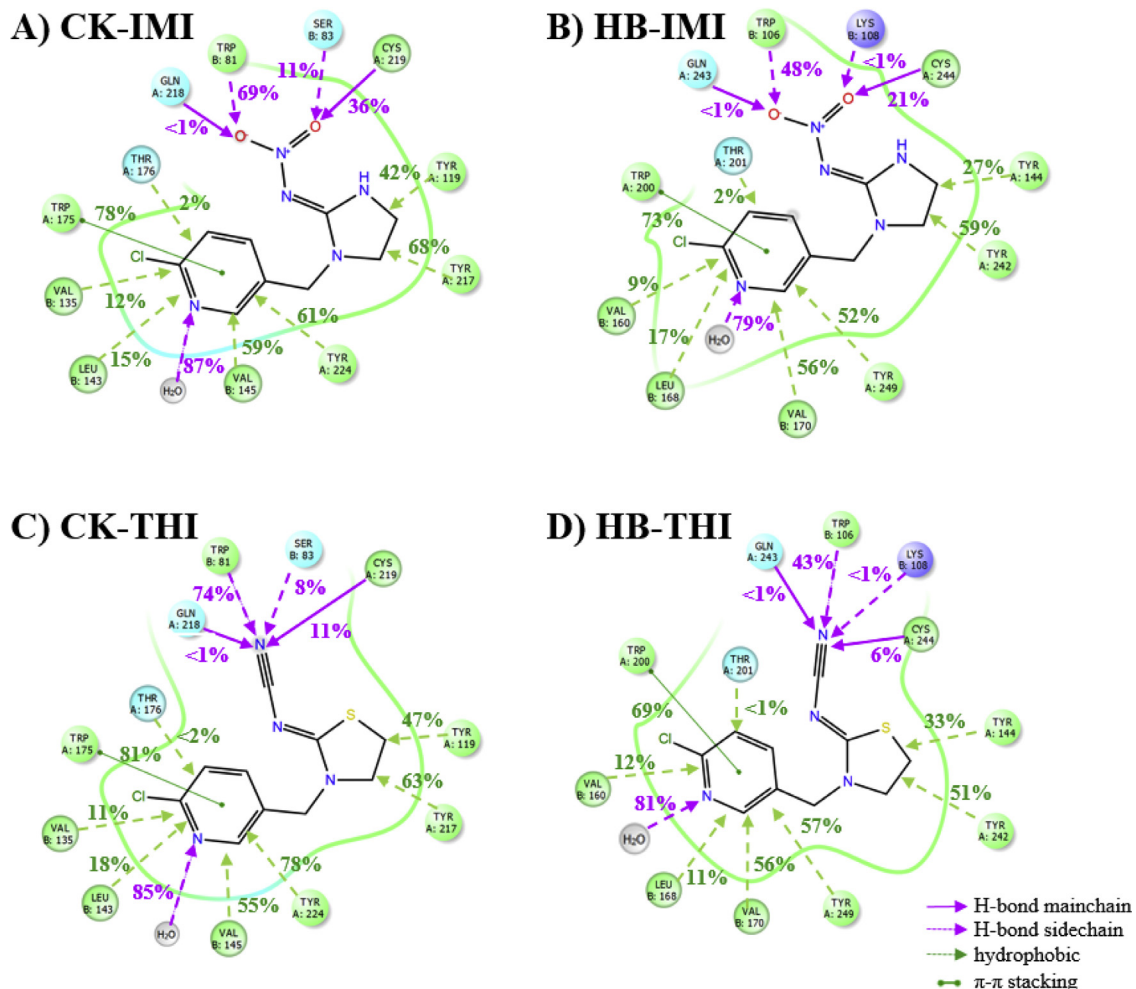


Fig. 9. The interaction profiles of neonicotinoids IMI and THI bound with α_6 cockroach and honeybee nAChR over the simulation time.

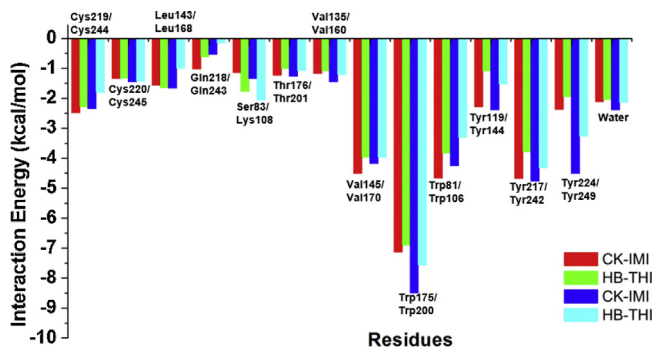


Fig. 10. Average interaction energies of binding site residues over the simulation time.

nAChRs. More precisely, the pyridine ring of IMI and THI interacts with 61% and 78% with Tyr224 and 52% and 57% with Tyr249 in cockroach and honeybee nAChRs. The hydrophobic residues Val145 and Val170 that belong to the apolar cluster of the binding site interact equally with both ligands in both nAChRs. In the same vein, Thr176/201, Val135/160 and Leu143/168 residues contribute to van der Waals interactions with the two neonicotinoids in cockroach and honeybee $\alpha 6$ nAChRs.

3.3.3. Binding energies

For a more quantitative analysis of the two neonicotinoids interactions in cockroach and honeybee $\alpha 6$ nAChRs, individual residue interaction energies have been calculated from the MD simulations using the DESMOND python tools (Fig. 10). The importance of non-specific interactions is confirmed, the contribution of the amino acids belonging to the aromatic clusters of the binding site Trp175/200, Trp81/106, Tyr119/144, Tyr217/242 and Tyr224/249 amounting for more than 70% of the average binding energy of the ligand. This behaviour is coherent with the well-known crucial role of aromatic residues in nAChR agonist binding pointed out originally by Van Arnam and Dougherty [59] through biochemical studies. Fig. 10 shows that the interaction energies of these aromatic residues are consistently stronger in cockroach than in honeybee nAChR. The loop B Trp175/Trp200 residue of cockroach and honeybee nAChRs (homolog to Trp147 of Ac-AChBP) bound with IMI and THI has the highest interaction energy among the other binding site residues. In particular, Trp175 of cockroach nAChR bound with THI has a binding energy of -9 kcal/mol. This result is coherent with experimental studies through NMR that have shown that the tryptophan residue of loop B plays a major role in ACh-nAChRs binding [60]. The other aromatic residues Trp217/242, Trp224/249 of loop C and Trp81/106 of loop D are involved in stronger interactions with the two neonicotinoids in the cockroach $\alpha 6$ compared to the honeybee nAChR. The involvement of these residues is in agreement with the study of Ohno et al. [58], who showed through SAR studies on several neonicotinoid analogues, the contribution of the homologous Tyr188 residue in the binding of these compounds to Ac-AChBP. Both the Cys219/244 and Cys220/245 residues exhibit van der Waals contacts with the neonicotinoids, the corresponding interaction energies being higher for IMI than THI. These results are also in line with the ones obtained in a recent investigation of the Ac-AChBP-IMI complex using a multi-quantum chemistry levels (QM/QM) hybrid methodology, which has pointed out the critical role of Trp147 and Cys190-191 residues for IMI binding [61]. The Val145/170 of loop E, which has been shown to be extremely sensitive to mutation [62] shows favourable interactions with both neonicotinoids bound to cockroach and honeybee $\alpha 6$ nAChRs. These combined modelling and biochemical studies have proven that mutation of Leu118 to Arginine and Lysine abolished IMI activity in $\alpha 7$ nAChRs [62]. Lastly, the present work

shows that the Thr176/201, Val135/160 and Leu143/168 residues have similar binding energies with the two neonicotinoids in both receptors.

The interaction energies of the non-conserved residues, however, are in contrast with respect to the results of our earlier analysis. Thus, the average binding energies of IMI and THI with the non-conserved Lys108 residue in honeybee $\alpha 6$ nAChR are respectively of -1.77 (IMI) and of -2.05 kcal/mol (THI), that is to say significantly greater than the corresponding values with Ser83 in cockroach $\alpha 6$ nAChR (-1.15 and -1.34 kcal/mol, respectively for IMI and THI). Nevertheless, these results agree with those obtained in a previous experimental study, which indicated that the presence of the positive charge moiety in loop D increased the sensitivity of the nAChRs to neonicotinoids [63]. In fact, the sidechain of Lys108 appears to contribute to the binding through numerous van der Waals contacts with the neonicotinoids. These interactions seem therefore stronger than the direct and water bridged contacts of the Ser83 OH group with nitro (IMI) and cyano (THI) groups. However, there is still a strong debate regarding the role of different amino acids having various electronic and physicochemical features, ranging from neutral to positively charge residues, in this particular position [64]. The hybrid vertebrate/insect nAChR has smaller and neutral residues such as Thr, Ser and Asn in loop D shows similar neonicotinoid potencies comparable to those observed for insects nAChRs, which possess positively charged residues such as Lysine and Arginine in loop D [56,65–67]. The selectivity studies on *Drosophila* nAChRs ($\alpha 2$ subunits) shows that neonicotinoids bind preferably to these subunits even though these receptors subunits have negatively charged residues in this loop [68]. Thus, the tick nAChR has a Glu81 residue at the specific position of loop D and modelling studies have concluded that the neonicotinoids are not selective for these nAChRs [69]. However, the Gln57 in the crystal structure of Ac-AChBP forms direct as well as water-mediated contact with the neonicotinoids [24]. The mutation of Gly57 to Gln increases the agonist efficacy to 7-fold in the mammalian muscle AChRs [70]. Despite the contradictions between the various modelling results, our work is in coherence with earlier biochemical and/or electrophysiological studies that have shown the importance of this position. Thus, the mutation of Thr59 to Lys or Asp in rat $\beta 2$ subunit of neuronal nAChR leads to a significant loss of agonist activity [71]. Similarly, the single mutation has least effect on the agonist activity on insects nAChRs compared to double mutation [64]. Although numerous and complementary experimental and theoretical studies have been carried out on these systems owing to their strong interest, a comprehensive understanding on the role of loop D residues in the selectivity for neonicotinoids is still required.

3.3.4. Role of non-conserved residues in the binding site

The dynamics of the apo and the ligand-bound structures reveal that the Ser83 and Lys108 residues of loop C in cockroach and honeybee $\alpha 6$ receptors have different roles in stabilizing the neonicotinoid bound conformation. The ammonium group of Lys108 forms an intramolecular ionic bridge with the carboxylate group of Asp218 and a H-bond interaction with the hydroxyl group of Thr87 with occupancies of 76% and 57%, respectively (see Fig. S7 in the SI). These interactions are present over the multiple runs in both apo and ligand-bound structures. The measurement of the $\text{C}\alpha$ atoms distances between Lys108 and Gln243 residues in honeybee $\alpha 6$ nAChR shows that loop C moves away from the initial position and induces an opening of the ligand binding site between the apo and complexed structures. Thus, the respective average $\text{C}\alpha$ distances between Lys108 and Gln243 residues in the apo and ligand bound complexes are of 12.5 \AA and 11.0 \AA (Fig. 11). The equivalent residues in Ac-AChBP are Gln57 and Ser189, the corresponding distances in ligand unoccupied and occupied structures being of 16.6 \AA and 9.5 \AA . However, the Ser83 residue in cockroach nAChR

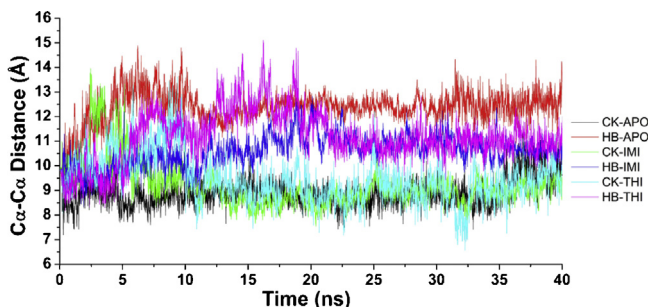


Fig. 11. C α atom distances between the loop C Gln218/Gln243 (principal chain) residues and the Ser83/Lys108 residues of loop D (complementary chain) in α 6 cockroach and honeybee nAChRs.

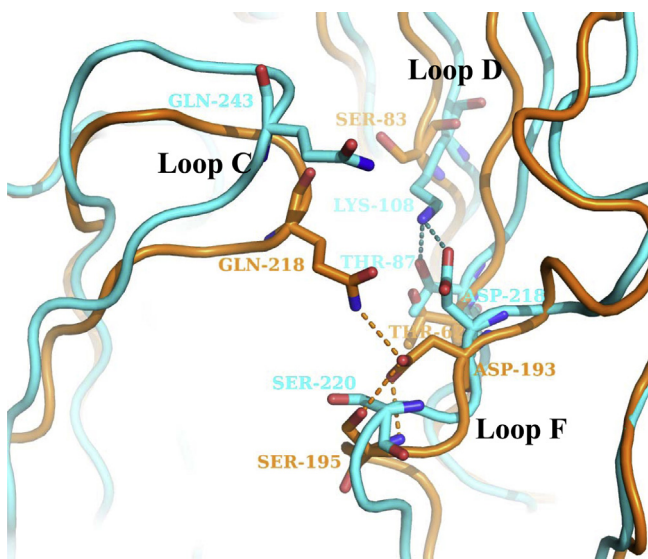


Fig. 12. Dynamics of loop C and loop D in apo structures of α 6 cockroach (orange) and honeybee (blue) nAChR. (For interpretation of reference to color in this figure legend, the reader is referred to the web version of this article.)

has a small side chain that does not form any interaction with equivalent residues Asp193 and Thr62. In turn, the amide group of Gln218 in loop C establishes a H-bond interaction with the carboxylate group of Asp193, this interaction being stable over the simulation time with an average occupancy of 67%. The formation of these intramolecular interactions decreases the C α distance between loop C and loop D residues (Fig. 12). In fact, the tightening of the loops between the two subunits stabilizes the neonicotinoid conformation and increases the binding affinity of neonicotinoids for cockroach compared to honeybee α 6 nAChRs. These findings are in agreement with the results obtained by Huang et al. on α 7 human nAChRs who demonstrated through molecular modelling studies that a corresponding intramolecular interaction between loop C Glu189 and Tyr168 residues improves agonist binding and the receptor activation [72].

4. Conclusions

In the present study, we have constructed the three-dimensional models of cockroach and honeybee α 6 nAChR homo-pentamer and docked the IMI and THI neonicotinoid ligands. MD simulations were carried out on the apo-structures and ligand-bound complexes in order to study the dynamics of various loops and to explore the interactions involved in neonicotinoid binding. The MD results show that the aromatic residues surrounding the ligand greatly stabilize the bound conformation through various

interactions. These interactions are found to be more specific for the ligands bound to the cockroach nAChR and thus appear to induce an increase of the corresponding sensitivity. The non-conserved Lys108 residue forms numerous van der Waals interactions with the neonicotinoids that appear more stable than the specific H-bonds established with the OH group of Ser83. However, the Lys108 residue is also shown to have a critical role in the dynamics of loop C, both in apo- and holo-structures, through electrostatic and/or H-bond interactions with neighbouring Asp218 and Gln243 residues. These interactions induce a partial opening of the binding site followed by a movement of loop C, leading to less favourable interactions with the neonicotinoids. In turn, the Gln218 of loop C interacts with Asp193 and Thr62 residues, these contacts prompting a tightening of loop C residues with the neonicotinoids in cockroach nAChR.

Consequently, the results reported herein highlight the role of conserved and non-conserved residues of cockroach and honeybee α 6 nAChRs as key determinants in the specificity for neonicotinoid binding. The detailed pictures of neonicotinoid binding provided in this work, validated through the good agreement with crystallographic data, pave the way towards the development of novel neonicotinoid ligands targeting specific components of the binding site.

Acknowledgements

J.-Y.L.Q. acknowledges the Région des Pays de la Loire for financial support in the framework of the ECRIN “Paris Scientifiques” Grant. This work was granted access to the HPC resources of [CCRT/CINES/IDRIS] under the allocation c2014085117 made by GENCI (Grand Equipment National de Calcul Intensif). The authors gratefully acknowledge the CCIPL (Centre de Calcul Intensif des Pays de la Loire) for grants of computer time and would also like to thank Aymeric Blondel for computational support.

Appendix A. Supplementary data

Supplementary data associated with this article can be found, in the online version, at <http://dx.doi.org/10.1016/j.jmgm.2014.10.018>.

References

- [1] A. AG., Chem. New Compound Rev. 30 (2012) 127–131.
- [2] P. Jeschke, R. Nauen, M.E. Beck, Nicotinic acetylcholine receptor agonists: a milestone for modern crop protection, Angew. Chem. Int. Ed. 52 (2013) 9464–9485.
- [3] M. Nys, D. Kesters, C. Ulens, Structural insights into Cys-loop receptor function and ligand recognition, Biochem. Pharmacol. 86 (2013) 1042–1053.
- [4] D. Lemoine, R. Jiang, A. Taly, T. Chataigneau, A. Specht, T. Grutter, Ligand-gated ion channels: new insights into neurological disorders and ligand recognition, Chem. Rev. 112 (2012) 6285–6318.
- [5] S.M. Sine, End-plate acetylcholine receptor: structure, mechanism, Pharmacol. Dis. Physiol. Rev. 92 (2012) 1189–1234.
- [6] D.A. Dougherty, Cys-loop neuroreceptors: structure to the rescue? Chem. Rev. 108 (2008) 1642–1653.
- [7] K. Matsuda, S.D. Buckingham, D. Kleier, J.J. Rauh, M. Grauso, D.B. Sattelle, Neonicotinoids: insecticides acting on insect nicotinic acetylcholine receptors, Trends Pharmacol. Sci. 22 (2001) 573–580.
- [8] K. Matsuda, M. Shimomura, M. Ihara, M. Akamatsu, D.B. Sattelle, Neonicotinoids show selective and diverse actions on their nicotinic receptor targets: electrophysiology, molecular biology, and receptor modelling studies, Biosci. Biotechnol. Biochem. 69 (2005) 1442–1452.
- [9] M. Tomizawa, J.E. Casida, Selective toxicity of neonicotinoids attributable to specificity of insect and mammalian nicotinic receptors, Annu. Rev. Entomol. 48 (2003) 339–364.
- [10] G.B. Wells, Structural answers and persistent questions about how nicotinic receptors work, Front. Biosci. 13 (2008) 5479–5510.
- [11] A. Miyazawa, Y. Fujiyoshi, N. Unwin, Structure and gating mechanism of the acetylcholine receptor pore, Nature 423 (2003) 949–955.
- [12] N. Unwin, Refined structure of the nicotinic acetylcholine receptor at 4 angstrom resolution, J. Mol. Biol. 346 (2005) 967–989.

- [13] N. Bocquet, L. Prado de Carvalho, J. Cartaud, J. Neyton, C. Le Poupon, A. Taly, T. Grutter, J.-P. Changeux, P.-J. Corringer, A prokaryotic proton-gated ion channel from the nicotinic acetylcholine receptor family, *Nature* 445 (2007) 116–119.
- [14] N. Bocquet, H. Nury, M. Baaden, C. Le Poupon, J.P. Changeux, M. Delarue, P.-J. Corringer, X-ray structure of a pentameric ligand-gated ion channel in an apparently open conformation, *Nature* 457 (2009) 111–114.
- [15] P.-J. Corringer, M. Baaden, N. Bocquet, M. Delarue, V. Dufresne, H. Nury, M. Prevost, C. Van Renterghem, Atomic structure and dynamics of pentameric ligand-gated ion channels: new insight from bacterial homologues, *J. Physiol.* 588 (2010) 565–572.
- [16] K. Brejc, W.J. van Dijk, R.V. Klaassen, M. Schuurmans, J. van der Oost, A.B. Smit, T.K. Sixma, Crystal structure of an ACh-binding protein reveals the ligand-binding domain of nicotinic receptors, *Nature* 411 (2001) 269–276.
- [17] C. Ulens, A. Akdemir, A. Jongejan, R. van Elk, S. Bertrand, A. Perrakis, R. Leurs, A.B. Smit, T.K. Sixma, D. Bertrand, I.J.P. de Esch, Use of acetylcholine binding protein in the search for novel alpha 7 nicotinic receptor ligands. In silico docking, pharmacological screening, and X-ray analysis, *J. Med. Chem.* 52 (2009) 2372–2383.
- [18] P. Rucktooja, A.B. Smit, T.K. Sixma, Insight in nAChR subtype selectivity from AChBP crystal structures, *Biochem. Pharmacol.* 78 (2009) 777–787.
- [19] P.H.N. Celie, S.E. Van Rossum-Fikkert, W.J. Van Dijk, K. Brejc, A.B. Smit, T.K. Sixma, Nicotine and carbamylcholine binding to nicotinic acetylcholine receptors as studied in AChBP crystal structures, *Neuron* 41 (2004) 907–914.
- [20] T.K. Sixma, A.B. Smit, Acetylcholine binding protein (AChBP): a secreted glial protein that provides a high-resolution model for the extracellular domain of pentameric ligand-gated ion channels, *Annu. Rev. Biophys. Biomol. Struct.* 32 (2003) 311–334.
- [21] S.B. Hansen, G. Sulzenbacher, T. Huxford, P. Marchot, P. Taylor, Y. Bourne, Structures of aplysia AChBP complexes with nicotinic agonists and antagonists reveal distinctive binding interfaces and conformations, *EMBO J.* 24 (2005) 3635–3646.
- [22] Y. Bourne, T.T. Talley, S.B. Hansen, P. Taylor, P. Marchot, Crystal structure of a Cbx-AChBP complex reveals essential interactions between snake a-neurotoxins and nicotinic receptors, *EMBO J.* 24 (2005) 1512–1522.
- [23] M. Tomizawa, J.E. Casida, Molecular recognition of neonicotinoid insecticides: the determinants of life or death, *Acc. Chem. Res.* 42 (2009) 260–269.
- [24] T.T. Talley, M. Harel, R.E. Hibbs, Z. Radic, M. Tomizawa, J.E. Casida, P. Taylor, Atomic interactions of neonicotinoid agonists with AChBP: molecular recognition of the distinctive electronegative pharmacophore, *Proc. Natl. Acad. Sci. U.S.A.* 105 (2008) 7606–7611.
- [25] K. Matsuda, S. Kanaoka, M. Akamatsu, D.B. Sattelle, Diverse actions and target-site selectivity of neonicotinoids: structural insights, *Mol. Pharmacol.* 76 (2009) 1–10.
- [26] M. Tomizawa, D. Maltby, T.T. Talley, K.A. Durkin, K.F. Medzihradzky, A.L. Burlingame, P. Taylor, J.E. Casida, Atypical nicotinic agonist bound conformations conferring subtype selectivity, *Proc. Natl. Acad. Sci. U.S.A.* 105 (2008) 1728–1732.
- [27] Z. Yixi, Z. Liu, Z. Han, F. Song, X. Yao, Y. Shao, J. Li, N.S. Millar, Functional co-expression of two insect nicotinic receptor subunits (N α 3 and N α 8) reveals the effects of a resistance-associated mutation (N α 3) on neonicotinoid insecticides, *J. Neurochem.* 110 (2009) 1855–1862.
- [28] Y. Huang, M.S. Williamson, A.L. Devonshire, J.D. Windass, S.J. Lansdell, N.S. Millar, Molecular characterization and imidacloprid selectivity of nicotinic acetylcholine receptor subunits from the peach-potato aphid *Myzus persicae*, *J. Neurochem.* 73 (1999) 380–389.
- [29] S.J. Lansdell, N.S. Millar, The influence of nicotinic receptor subunit composition upon agonist, a-bungarotoxin and insecticide (imidacloprid) binding affinity, *Neuropharmacology* 39 (2000) 671–679.
- [30] S.J. Lansdell, N.S. Millar, Molecular characterization of D alpha 6 and D alpha 7 nicotinic acetylcholine receptor subunits from *Drosophila*: formation of a high-affinity alpha-bungarotoxin binding site revealed by expression of subunit chimeras, *J. Neurochem.* 90 (2004) 479–489.
- [31] Z.W. Liu, M.S. Williamson, S.J. Lansdell, I. Denholm, Z.J. Han, N.S. Millar, A nicotinic acetylcholine receptor mutation conferring target-site resistance to imidacloprid in *Nilaparvata lugens* (brown planthopper), *Proc. Natl. Acad. Sci. U.S.A.* 102 (2005) 8420–8425.
- [32] Z. Liu, Z. Han, Y. Zhang, F. Song, X. Yao, S. Liu, J. Gu, N.S. Millar, Heteromeric co-assembly of two insect nicotinic acetylcholine receptor alpha subunits: influence on sensitivity to neonicotinoid insecticides, *J. Neurochem.* 108 (2009) 498–506.
- [33] S.J. Lansdell, T. Collins, J. Goodchild, N.S. Millar, The *Drosophila* nicotinic acetylcholine receptor subunits D α 5 and D α 7 form functional homomeric and heteromeric ion channels, *BMC Neurosci.* 13 (2012) 1–11, Article number 73.
- [34] D. Bertrand, M. Ballivet, M. Gomez, S. Bertrand, B. Phannavong, E.D. Gundelfinger, Physiological properties of neuronal nicotinic receptors reconstituted from the vertebrate beta 2 subunit and *Drosophila* alpha subunits, *Eur. J. Neurosci.* 6 (1994) 869–875.
- [35] T.T. Talley, M. Harel, R.E. Hibbs, Z. Radic, M. Tomizawa, J.E. Casida, P. Taylor, Atomic interactions of neonicotinoid agonists with AChBP: molecular recognition of the distinctive electronegative pharmacophore, *Proc. Natl. Acad. Sci. U.S.A.* 105 (2008) 7606–7611.
- [36] E. Gasteiger, A. Gattiker, C. Hoogland, I. Ivanyi, R.D. Appel, A. Bairoch, ExPASy: the proteomics server for in-depth protein knowledge and analysis, *Nucl. Acids Res.* 31 (2003) 3784–3788.
- [37] S.F. Altschul, W. Gish, W. Miller, E.W. Myers, D.J. Lipman, Basic local alignment search tool, *J. Mol. Biol.* 215 (1990) 403–410.
- [38] M. Tomizawa, J.E. Casida, Molecular recognition of neonicotinoid insecticides: the determinants of life or death, *Acc. Chem. Res.* 42 (2008) 260–269.
- [39] H.M. Berman, T. Battistuz, T. Bhat, W.F. Bluhm, P.E. Bourne, K. Burkhardt, Z. Feng, G.L. Gilliland, L. Iype, S. Jain, P. Fagan, J. Marvin, D. Padilla, V. Ravichandran, B. Schneider, N. Thanki, H. Weissig, J. Westbrook, C. Zardecki, The protein data bank, *Acta Crystallogr. Sect. D: Biol. Crystallogr.* 58 (2002) 899–907.
- [40] Schrödinger Release 2014-1: Prime, version 3.5, Schrödinger, LLC, New York, NY, 2014.
- [41] Schrödinger Release 2014-1, Schrödinger, LLC, New York, NY, 2014.
- [42] V.B. Chen, W.B. Arendall, J.J. Headd, D.A. Keedy, R.M. Immormino, G.J. Kapral, L.W. Murray, J.S. Richardson, D.C. Richardson, MolProbity: all-atom structure validation for macromolecular crystallography, *Acta Crystallogr. Sect. D: Biol. Crystallogr.* 66 (2009) 12–21.
- [43] Schrödinger Release 2014-1: LigPrep, version 2.9, Schrödinger, LLC, New York, NY, 2014.
- [44] Schrödinger Release 2014-1: ConfGen, version 2.7, Schrödinger, LLC, New York, NY, 2014.
- [45] R.A. Friesner, J.L. Banks, R.B. Murphy, T.A. Halgren, J.J. Klicic, D.T. Mainz, et al., Glide: a new approach for rapid, accurate docking and scoring. 1. Method and assessment of docking accuracy, *J. Med. Chem.* 47 (2004) 1739–1749.
- [46] R.A. Friesner, R.B. Murphy, M.P. Repasky, L.L. Frye, J.R. Greenwood, T.A. Halgren, P.C. Sanschagrin, D.T. Mainz, Extra precision glide: docking and scoring incorporating a model of hydrophobic enclosure for protein-ligand complexes, *J. Med. Chem.* 49 (2006) 6177–6196.
- [47] Schrödinger Release 2014-1: Desmond Molecular Dynamics System, version 3.7, D. E. Shaw Research, New York, NY, 2014. Maestro-Desmond Interoperability Tools, version 3.7, Schrödinger, New York, NY, 2014.
- [48] K. Vanommeslaeghe, E. Hatcher, C. Acharya, S. Kundu, S. Zhong, J. Shim, E. Darrian, O. Guvenc, P. Lopes, I. Vorobyov, A.D. Mackerell Jr., CHARMM general force field: a force field for drug-like molecules compatible with the CHARMM all-atom additive biological force fields, *J. Computat. Chem.* 31 (2010) 671–690.
- [49] Schrödinger Release 2014-1: Maestro, version 9.7, Schrödinger, LLC, New York, NY, 2014.
- [50] T. Darden, D. York, L. Pedersen, Particle mesh Ewald: an N log (N) method for Ewald sums in large systems, *J. Chem. Phys.* 98 (1993) 10089–10092.
- [51] V. Kräutler, W.F. van Gunsteren, P.H. Hünenberger, A fast SHAKE algorithm to solve distance constraint equations for small molecules in molecular dynamics simulations, *J. Computat. Chem.* 22 (2001) 501–508.
- [52] J. Liang, H. Naveed, D. Jimenez-Morales, L. Adamian, M. Lin, Computational studies of membrane proteins: models and predictions for biological understanding, *Biochim. Biophys. Acta (BBA): Biomemb.* 1818 (2012) 927–941.
- [53] W.L. Jorgensen, D.S. Maxwell, J. Tirado-Rives, Development and testing of the OPLS all-atom force field on conformational energetics and properties of organic liquids, *J. Am. Chem. Soc.* 118 (1996) 11225–11236.
- [54] G. Ramachandran, C.t. Ramakrishnan, V. Sasisekharan, Stereochemistry of polypeptide chain configurations, *J. Mol. Biol.* 7 (1963) 95–99.
- [55] M. Tomizawa, T.T. Talley, D. Maltby, K.A. Durkin, K.F. Medzihradzky, A.L. Burlingame, P. Taylor, J.E. Casida, Mapping the elusive neonicotinoid binding site, *Proc. Natl. Acad. Sci. U.S.A.* 104 (2007) 9075–9080.
- [56] J. Tan, J.J. Galligan, R.M. Hollingworth, Agonist actions of neonicotinoids on nicotinic acetylcholine receptors expressed by cockroach neurons, *Neurotoxicology* 28 (2007) 829–842.
- [57] S. Amiri, M.S. Sansom, P.C. Biggin, Molecular dynamics studies of AChBP with nicotine and carbamylcholine: the role of water in the binding pocket, *Protein Eng. Des. Select.* 20 (2007) 353–359.
- [58] I. Ohno, M. Tomizawa, K.A. Durkin, J.E. Casida, S. Kagabu, Neonicotinoid substituents forming a water bridge at the nicotinic acetylcholine receptor, *J. Agric. Food Chem.* 57 (2009) 2436–2440.
- [59] E.B. Van Arnam, D.A. Dougherty, Functional probes of drug-receptor interactions implicated by structural studies: cys-loop receptors provide a fertile testing ground: miniperspective, *J. Med. Chem.* 57 (2014) 6289–6300.
- [60] Y. Fraenkel, J.M. Gershoni, G. Navon, Acetylcholine interactions with tryptophan-184 of the α -subunit of the nicotinic acetylcholine receptor revealed by transferred nuclear Overhauser effect, *FEBS Lett.* 291 (1991) 225–228.
- [61] J.P. Ceroñ-Carrasco, D. Jacquemin, J.r.m. Graton, S. Thany, J.-Y. Le Questel, New insights on the molecular recognition of imidacloprid with *Aplysia californica* AChBP: a computational study, *J. Phys. Chem. B* 117 (2013) 3944–3953.
- [62] S. Amiri, M. Shimomura, R. Vijayan, H. Nishiwaki, M. Akamatsu, K. Matsuda, A.K. Jones, M.S.P. Sansom, P.C. Biggin, Sattelle, B.A. David, role for Leu118 of loop E in agonist binding to the α 7 nicotinic acetylcholine receptor, *Mol. Pharmacol.* 73 (2008) 1659–1667.
- [63] M. Tomizawa, D.L. Lee, J.E. Casida, Neonicotinoid insecticides: molecular features conferring selectivity for insect versus mammalian nicotinic receptors, *J. Agric. Food Chem.* 48 (2000) 6016–6024.
- [64] M. Shimomura, M. Yokota, M. Ihara, M. Akamatsu, D.B. Sattelle, K. Matsuda, Role in the selectivity of neonicotinoids of insect-specific basic residues in loop D of the nicotinic acetylcholine receptor agonist binding site, *Mol. Pharmacol.* 70 (2006) 1255–1263.
- [65] F. Song, Z. You, X. Yao, J. Cheng, Z. Liu, K. Lin, Specific loops D, E and F of nicotinic acetylcholine receptor β 1 subunit may confer imidacloprid selectivity between *Myzus persicae* and its predatory enemy *Pardosa pseudoannulata*, *Insect Biochem. Mol. Biol.* 39 (2009) 833–841.
- [66] X. Yao, F. Song, F. Chen, Y. Zhang, J. Gu, S. Liu, Z. Liu, Amino acids within loops D, E and F of insect nicotinic acetylcholine receptor β subunits influence neonicotinoid selectivity, *Insect Biochem. Mol. Biol.* 38 (2008) 834–840.

- [67] X. Yao, F. Song, Y. Zhang, Y. Shao, J. Li, Z. Liu, Nicotinic acetylcholine receptor $\beta 1$ subunit from the brown planthopper, *Nilaparvata lugens*: A-to-I RNA editing and its possible roles in neonicotinoid sensitivity, *Insect Biochem. Mol. Biol.* 39 (2009) 348–354.
- [68] M. Tomizawa, N. Zhang, K.A. Durkin, M.M. Olmstead, J.E. Casida, The neonicotinoid electronegative pharmacophore plays the crucial role in the high affinity and selectivity for the *Drosophila* nicotinic receptor: an anomaly for the nicotinoid cation- π interaction model, *Biochemistry* 42 (2003) 7819–7827.
- [69] L. Erdmanis, A.O. O'Reilly, M.S. Williamson, L.M. Field, A. Turberg, B.A. Wallace, Association of neonicotinoid insensitivity with a conserved residue in the loop D binding region of the tick nicotinic acetylcholine receptor, *Biochemistry* 51 (2012) 4627–4629.
- [70] M. Bartos, K.L. Price, S.C. Lummis, C. Bouzat, Glutamine 57 at the complementary binding site face is a key determinant of morantel selectivity for $\alpha 7$ nicotinic receptors, *J. Biol. Chem.* 284 (2009) 21478–21487.
- [71] M.J. Parker, S.C. Harvey, C.W. Luetje, Determinants of agonist binding affinity on neuronal nicotinic receptor β subunits, *J. Pharmacol. Exp. Ther.* 299 (2001) 385–391.
- [72] X. Huang, F. Zheng, C. Stokes, R.L. Papke, C.G. Zhan, Modelling binding modes of $\alpha 7$ nicotinic acetylcholine receptor with ligands: the roles of Gln117 and other residues of the receptor in agonist binding, *J. Med. Chem.* 51 (2008) 6293–6302.